



Joint Modeling for MC-TDMA and Beamforming in mmWave Communications

Kwame S Ibwe

College of Information and Communication Technologies, University of Dar es Salaam

P. O. Box 33335, Dar es Salaam, Tanzania

Corresponding author e-mail: kwame.ibwe@gmail.com

Received 12 Oct 2024, Revised 27 Jan 2025, Accepted 20 March 25, Published 14 April 2025

<https://dx.doi.org/10.4314/tjs.v51i1.9>

Abstract

The increasing demand for ultra-high data rates and low-latency communication in next-generation wireless networks has led to the exploration of millimeter-wave (mmWave) frequency bands. These frequency bands offer significant bandwidth but are challenged by severe path loss, high susceptibility to blockage, and complex channel conditions. To address these challenges, a joint system modeling framework that integrates multicarrier time-division multiple access (MC-TDMA) with beamforming techniques is introduced. This study presents an analytical model that combines MC-TDMA's flexible time-slot allocation with the high directionality and interference mitigation capabilities of beamforming, tailored to the unique characteristics of mmWave channels. Two optimization algorithms are proposed based on dynamic resource allocations for time slot allocations and hybrid beamforming respectively. Simulations experiments are performed under realistic propagation conditions, considering number of base station antennas, radio frequency (RF) chains, number of users and channel paths. Results demonstrate superior performance over existing schemes. The proposed schemes are verified to have smaller spectral efficiency gaps when compared to the fully-digital beamforming method. The findings offer a practical solution for high-capacity, low-latency communication in dense and dynamic mmWave environments, paving the way for more efficient next-generation networks design.

Keywords: Beamforming; Modeling; mmWave; MC-TDMA; Spectral Efficiency; 5G Networks

Introduction

The rapid advancement of wireless communication technologies has introduced new paradigms such as 5G, with visions of 6G on the horizon (Chen et al. 2023). These next-generation networks promise to meet the ever-growing demands for ultra-high data rates, low-latency communication, and massive connectivity (Ji et al. 2018). To achieve these ambitious goals, researchers have turned their attention to higher frequency bands, specifically millimeter-wave (mmWave) and Terahertz (THz) frequencies, which offer abundant bandwidth resources (Golos et al. 2023, Yong et al. 2023, Xue et al. 2024).

Frequencies in the mmWave (30-300 GHz) and THz (0.1-10 THz) ranges are particularly attractive due to their ability to support data rates in the multi-gigabit-per-second range (Moltchanov et al. 2022). However, their adoption presents significant challenges, particularly related to propagation losses, high susceptibility to blockages, and increased sensitivity to environmental changes (Chen et al. 2022, Alsaedi et al. 2023).

Large scale antennas array technology like massive multiple input multiple output (MIMO) systems can be used to increase capacity, reliability and spectral efficiency of the mmWave communications (Shareef and

Al-Kindi 2023). The challenge of implementing large number of antennas at the user terminal for lower frequency of operation is solved by the application of mmWave frequencies (Raheja et al. 2019). It is observed that the size of 4x4 uniform planar array (UPA) at 5 GHz is 80 cm² (Naik and Virani 2022). At 28 GHz the size is reduced to 2.6 cm². This allows a greater number of UPAs to be implemented in 28 GHz and provide beamforming (Verma and Mishra 2022). Despite the fact that mmWave provides more accurate beamforming, the narrow beamwidth required to overcome propagation issues make the system highly sensitive to beam misalignment, particularly in dynamic environments such as vehicular communication systems (Yuan et al. 2023). Therefore, efficient techniques to mitigate these propagation challenges are essential for enabling robust and reliable communication in mmWave systems (Busari et al. 2018). To address these challenges, one promising approach is the integration of multicarrier (MC) transmission schemes, time-division multiple access (TDMA) and advanced beamforming techniques. The MC-TDMA offers flexible resource allocation by dividing time and frequency resources among users, making it suitable for managing the wide bandwidth available at higher frequencies (Huang et al. 2023). Meanwhile, beamforming concentrates signal energy into highly directional beams, compensating for the high path loss at mmWave frequencies to enhance system capacity, improve spectral efficiency, and ensure better coverage (Kutty and Sen 2016, Ullah et al. 2022, Beiranvand et al. 2023).

However, combining MC-TDMA with beamforming introduces new complexities in the system modeling (Huang et al. 2023). Existing system models for mmWave frequencies often focus on either beamforming or multicarrier transmission in isolation, leaving a gap in the understanding of their combined effects (Moltchanov et al. 2022, Yusof et al. 2023). Furthermore, the joint impact of these technologies on key performance indicators, such as bit error rate (BER), spectral efficiency, and outage

probability, under realistic channel conditions remains underexplored. This paper aims to fill this gap by developing an analytical model for joint system that integrates MC-TDMA with beamforming in mmWave communications. The proposed model accounts for key propagation characteristics of mmWave frequencies, including path loss, small-scale fading, and beam misalignment. The performance metrics such as BER, system capacity, and spectral efficiency are derived to assess the effectiveness of this joint approach in various operating environments. The model is validated through extensive simulations and compared with existing schemes. The contribution of the paper is twofold: a joint analytical system model that incorporates MC-TDMA and beamforming for mmWave communication systems is derived; time-slot/subcarrier allocation and hybrid precoding optimization algorithms are designed to maximize systems' spectral efficiency.

The millimeter-wave (mmWave) frequency band has gained popularity in recent years due to its potential for providing ultra-high data rates and supporting next-generation wireless networks such as 5G and beyond (Busari et al. 2018). Several research efforts have been dedicated to understanding and addressing the challenges posed by the unique characteristics of mmWave communications, such as severe path loss, high susceptibility to blockages, and propagation sensitivity (Li et al. 2022). To mitigate these challenges, the use of beamforming techniques, multicarrier (MC) systems, and massive multiple input multiple output (MIMO) technologies have been explored extensively (Getahun and Rajkumar 2023).

Beamforming plays a crucial role in overcoming the high path loss associated with mmWave frequencies by directing energy into highly focused beams (Soumya et al. 2023). Traditional fully-digital beamforming, where each antenna element is controlled individually, has been shown to achieve optimal performance in terms of spectral efficiency and interference management (Mezzavilla et al. 2018). However, its complexity and power consumption grow

prohibitively large as the number of antennas increases, especially in massive MIMO systems (Kutty and Sen 2016). Hybrid beamforming has emerged as a practical alternative that reduces hardware complexity by combining digital and analog beamforming (Teng et al. 2021). Numerous studies have proposed different hybrid beamforming designs to balance performance and cost, including dynamic hybrid precoding (Alkhateeb et al. 2013) and partially-connected architectures (Song et al. 2020), manifold optimization (Du et al. 2019) and block diagonalization (Shareef and Al-Kindi 2023). These approaches achieve near-optimal performance at a fraction of the complexity of fully-digital beamforming.

The combination of multicarrier transmission schemes with mmWave communications has also been extensively studied (Shareef and Al-Kindi 2023). Orthogonal Frequency Division Multiplexing (OFDM) is a widely used multicarrier scheme that offers robustness against frequency-selective fading, making it well-suited for mmWave channels (Basha et al. 2023). However, OFDM's high peak-to-average power ratio (PAPR) poses challenges for mmWave systems. To address this, several studies have investigated alternative multicarrier schemes, including filter bank multicarrier (FBMC) (Farhang-Boroujeny 2011) and generalized frequency division multiplexing (GFDM) (Wang et al. 2023), which offer lower PAPR and better spectral efficiency. Time-division multiple access (TDMA) has also been employed to manage the allocation of time and frequency resources in mmWave systems (Zhang and Zhu 2020). Studies have demonstrated that integrating TDMA with beamforming can enhance system capacity and reduce interference in dense environments (Bahbahani et al. 2023, Khaled et al. 2023). Although some research has focused on the independent use of either beamforming or multicarrier schemes in mmWave, the joint modeling of MC-TDMA and beamforming has not been thoroughly explored.

Despite the progress in beamforming and MC systems, the combination of these two

techniques remains underexplored in the context of mmWave communications (Khudhair and Singh 2021). The integration of MC-TDMA with beamforming can potentially offer more flexible and efficient resource allocation (Rajashekar et al. 2019). However, this integration introduces additional challenges, particularly in managing the complexity of hybrid beamforming and ensuring efficient time-slot and subcarrier allocation (Hamid et al. 2023). Existing works have focused either on the optimization of beamforming techniques (Sohrabi and Yu 2017) or on multicarrier systems (Khudhair and Singh 2021), leaving a gap in the comprehensive understanding of their combined effects. Recent efforts have started to explore the potential of combining MC and beamforming techniques to improve system performance. For example, studies have examined the performance of MC systems under different hybrid beamforming architectures (Eisenbeis et al. 2021), but few have considered the impact of joint resource allocation. Furthermore, while several works have explored mmWave channel models (Rappaport et al. 2015), most focus on point-to-point systems rather than multiple access networks (Chen et al. 2021). The joint modeling of MC-TDMA and beamforming, as proposed in this paper, offers a novel approach to address these gaps by optimizing both resource allocation and beamforming under realistic mmWave channel conditions.

Materials and Methods

System and Channel Model

In the proposed MC-TDMA scheme, users are assigned orthogonal time slots across multiple subcarriers. Figure 1 shows the MC-TDMA base station (BS) transmitter structure with hybrid beamforming equipped with U radio frequency (RF) chains and M antennas. The system operates over a total bandwidth B , which is divided into N subcarriers each with

bandwidth $\Delta f = \frac{B}{N}$ are used for data

transmission where U single-antenna users are simultaneously served on the entire band. For each time slot T_s the subcarriers are assigned

to users according to the TDMA scheduling. At any given time slot T_s a user is allowed exclusive access to a set of subcarriers,

ensuring that no inter-user interference occurs within that time slot.

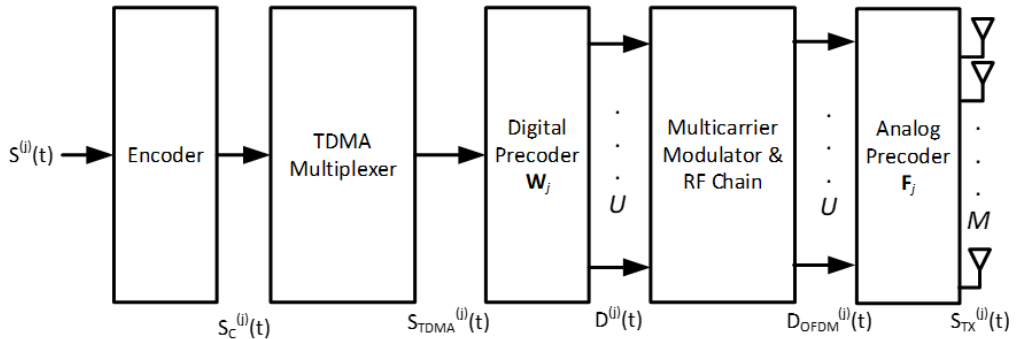


Figure 1: MC-TDMA Transmitter Structure with Hybrid Beamforming

Let the digital signal of j -th user be represented by

$$S^{(j)}(t) = \sum_k a_k^{(j)} \delta(t - kT) \quad (1)$$

where $a_k^{(j)}$ is the k -th binary antipodal symbol generated by user j and T stand for time period between symbols.

The symbols for the unique signals are arranged in terms of groups for N_{bps} in a single time slot of duration T_s . Time slots are arranged in frames of duration T_F .

$$S_C^{(j)}(t) = \sum_m \sum_{k=1}^{N_{bps}} a_{k+mN_{bps}}^{(j)} \delta(t - kT_C - mT_F) \quad (2)$$

where T_C stand for time interval between symbols after compression. The position in time for each group is modified in accordance to the TDMA code which is assigned to the user. In other words, the TDMA code specifies which slot within each frame should be occupied by the user. By assigning each user with a particular code, equation 2 becomes:

$$S_{TDMA}^{(j)}(t) = \sum_m \sum_{k=1}^{N_{bps}} a_{k+mN_{bps}}^{(j)} \delta(t - kT_C - C_m^{(j)}T_s - mT_F) \quad (3)$$

where $C_m^{(j)}$ is the TDMA code allocated to user j for the m -th frame.

The digital precoding is applied in the baseband domain before multicarrier modulation stage. \mathbf{W}_j is the digital precoding matrix for user j , which has dimensions $U \times U$, where U is the number of RF chains. The digital precoded signal for user j is obtained as

$$D^{(j)}(t) = \mathbf{W}_j S_{TDMA}^{(j)}(t) \quad (4)$$

where $\mathbf{W}_j = [w_{1j}, w_{2j}, \dots, w_{Mj}] \in \mathbb{C}^{U \times U}$ represent digital precoder for user j . The multicarrier block transforms the signal in equation 4 into

$$D_{OFDM}^{(j)}(t) = \sum_{k=0}^{N-1} D^{(j)}(t) e^{j2\pi f_k t} \quad (5)$$

$$D_{OFDM}^{(j)}(t) = \sum_{k=0}^{N-1} \mathbf{W}_j S_{TDMA}^{(j)}(t) e^{j2\pi f_k t} \quad (6)$$

$$D_{OFDM}^{(j)}(t) = \sum_{k=0}^{N-1} \sum_m \sum_{l=1}^{N_{bps}} \mathbf{W}_j a_{k+mN_{bps}}^{(j)} \delta(t - kT_C - C_m^{(j)}T_s - mT_F) e^{j2\pi f_k t} \quad (7)$$

The analog precoder $\mathbf{F}_j = [f_{1j}, f_{2j}, \dots, f_{Uj}]$ with dimensions $M \times U$ is applied at the RF stage using phase shifters. The analog precoder modifies the signal across the antenna array for beamforming. The signal generated for user j is presented as

$$S_{TX}^{(j)}(t) = \mathbf{F}_j D_{OFDM}^{(j)}(t) \quad (8)$$

$$S_{TX}^{(j)}(t) = \sum_{k=0}^{N-1} \mathbf{F}_j \mathbf{W}_j S_{TDMA}^{(j)}(t) e^{j2\pi f_k t} \quad (9)$$

The baseband signal in equation 9 is up converted by a power amplifier at a carrier frequency f_c to produce a passband signal presented as

$$S_{pTX}^{(j)}(t) = S_{TX}^{(j)}(t) e^{j2\pi f_c t} \quad (10)$$

$$S_{pTX}^{(j)}(t) = \sum_{k=0}^{N-1} \sum_m \sum_{l=1}^{N_{bps}} \mathbf{F}_j \mathbf{W}_j a_{k+mN_{bps}}^{(j)} \delta(t - kT_C - C_m^{(j)}T_s - mT_F) e^{j2\pi f_k t} e^{j2\pi f_c t} \quad (11)$$

The narrowband mmWave channel is assumed to be sparse scattering with L multipath components. Each of the components is characterized by a gain α_l and angular parameters $\theta_{r,l}$ and $\theta_{t,l}$ (angles of arrival and departure). The a_r and a_t are receive and transmit array response vectors respectively. The channel matrix $\mathbf{H}_j = [h_j[1], h_j[2], \dots, h_j[U]] \in \mathbb{C}^{M \times U}$ is represented as

$$\mathbf{H}_j = \sum_{l=1}^L \alpha_{j,l} a_r(\theta_{r,l}) a_t(\theta_{t,l})^H e^{j2\pi f_c \tau_l} \quad (12)$$

The received signal for user j is now presented as

$$S_{RX}^{(j)} = \mathbf{H}_j^H \mathbf{F}_j \mathbf{W}_j S_{TDMA}^{(j)} + n_j \quad (13)$$

where n_j is additive white Gaussian noise for user j and $n_j \sim \mathcal{CN}(0_N, P_n I_N)$ in which P_n is the noise power. The received signal of all active users in the MC-TDMA system can also be presented as

$$S_{RX}(t) = \sum_{j=1}^U \sum_{k=0}^{N-1} \sum_m \sum_{l=1}^{N_{bps}} \mathbf{H}_j^H \mathbf{F}_j \mathbf{W}_j \sqrt{\frac{2P_j}{N}} a_{l+mN_{bps}}^{(j)} \cos \left[2\pi \left(f_c + \frac{k}{T_C} \right) t \right] \cdot C_m^j \cdot \chi(t - lT_C) + n(t) + \xi(t)$$

where $\chi(t)$ indicates the rectangular pulse defined in $[0, T_C]$, P_j is the j -th user signal power and lastly $\xi(t)$ indicates user interference.

In this work the fully connected structure of the hybrid precoding is considered in which each RF chain drives all the antennas. Now, the received signal of the j -th user at subcarrier k is given as

$$S_{RX}^{(j)}[k] = h_j^H[k] \mathbf{FWS}_{TDMA}^{(j)}[k] + n_j[k] \tag{15}$$

To characterize the practical scattering of mmWave channels, in this work the geometric model presented in (Rappaport et al. 2015) is adopted. Since the number of users corresponds to the number of antennas used, the subscript j can be interchanged with U . It is also assumed that the channels between the

BS and users have the same number of paths. For the u -th user, the path time delay is given as $\tau_{u,l} \in \mathbb{R}$, angle of arrival and angle of departure $\theta_{r,l}, \theta_{t,l} \in [0, 2\pi]$. The channel vector for u -th user is given as

$$h_u[k] = \sqrt{\frac{M}{L}} \sum_{n=1}^{N_c-1} \left[e^{-j \frac{2\pi k n}{N}} \sum_{l=1}^L \alpha_{u,l} \chi(nT_s - \tau_{u,l}) a_{u,l} \right] \tag{16}$$

where N_c denotes the number of delay taps, $\chi(\tau)$ is the pulse shaping filter, $a_{u,l}$ denotes the antenna array response vector of the BS.

Objective Function

The problem of interest in this work is to maximize the total data rate for all users in a multi-user MC-TDMA system with hybrid beamforming, while ensuring that each user meets a minimum required signal to interference plus noise ratio (SINR). The frequency-selective nature of mmWave

channels, combined with the use of time-slot and subcarrier multiplexing, poses challenges in maintaining high data rates, particularly in the presence of path loss, fading, and beam misalignment. In this case, the data rate for user u on subcarrier k in the MC-TDMA system with hybrid beamforming is presented as

$$R_u[k] = \Delta f_k \log_2(1 + SINR_u[k]) \tag{17}$$

where Δf_k is the bandwidth of subcarrier k and $SINR_u[k]$ is the signal to interference plus noise ratio for user u on subcarrier k . The SINR on user u on the subcarrier k is determined by the power allocation, beamforming gain and interference from other users and subcarriers as well as noise. The SINR is defined as

$$SINR_u[k] = \frac{\mathbf{Z}_{u,k} P_u \left| \mathbf{F}_u^H \mathbf{W}_u h_u(\theta_{\text{offset},u}) \right|^2}{\sum_{i \neq u} \mathbf{Z}_{u,i} P_i \left| \mathbf{F}_i \mathbf{W}_i h_u(\theta_{\text{offset},i}) \right|^2 + \sigma_n^2 + \eta_u} \quad (18)$$

where P_u is power allocated to user u , $h_u(\theta_{\text{offset},u})$ is the channel vector with beam misalignment $\theta_{\text{offset},u}$, σ_n^2 is the noise power, $\mathbf{Z}_{u,k}$ is the time slot assignment matrix and $\xi_u = \sum_{i \neq u} P_i \left| \mathbf{F}_i \mathbf{W}_i h_u(\theta_{\text{offset},i}) \right|^2$ is the interference power from user i . Now, for the proposed MC-TDMA system, the objective function is written as

$$\max_{\mathbf{F}, \mathbf{W}, \mathbf{P}, \mathbf{Z}} \sum_{k=1}^N \sum_{u=1}^U \log_2 \left(1 + \frac{SINR_u[k]}{\sigma_n^2} \right) \quad (19)$$

$$s.t. \quad \left\| \mathbf{F} \mathbf{W}_u[k] \right\|_F \leq P_{\max}, \quad \forall 1 \leq u \leq U, 1 \leq k \leq N$$

$$\left| f_{u,i} \right| = \frac{1}{\sqrt{M}}, \quad \forall 1 \leq i \leq M, 1 \leq u \leq U$$

$$\sum_{k=1}^N z_{u,k} = 1, \quad \forall u$$

To solve the objective problem, design strategies are presented in this work. It is assumed that the perfect channel state information (CSI) is available in order to study the performance limits of the time division multiplexing and hybrid beamforming structure.

Optimization Algorithm

The main challenge of the problem presented in equation 19 is solving for multivariable i.e. $\mathbf{F}, \mathbf{W}, \mathbf{Z}$. In this work maximization algorithms for time-slot/subcarrier allocation and hybrid precoding to maximize the overall data rate for MC-TDMA system are presented. However, instead of solving the original optimization

problem for the three variables, the presented algorithms separate the problem into optimization functions for time-slot allocation and hybrid precoding.

Time Slot Assignment Design

To design the time-slot and subcarrier assignment matrix \mathbf{Z} so that it maximizes the achievable data rate in the proposed MC-TDMA system, the dynamic resource allocation method is applied. The matrix \mathbf{Z} represents how time slots and subcarriers are allocated to users across the frequency and time domains. Since the objective is to maximize the sum data rate of all users across time-slots and subcarriers, therefore the objective function is presented as

$$\max_{\mathbf{F}, \mathbf{W}, \mathbf{P}, \mathbf{Z}} \sum_{k=1}^N \sum_{u=1}^U \log_2 \left(1 + \frac{P_u[k] \left| h_u[k]^H \mathbf{W} \mathbf{F}_u[k] \right|^2}{\xi_u[k] + \sigma_n^2} \right) \quad (20)$$

where $h_u[k]$ is the channel vector for user u on subcarrier k , \mathbf{W} is the analog precoding matrix, $\mathbf{F}_u[k]$ is the digital precoding for user u on subcarrier k , $P_u[k]$ is the power allocation to user u on subcarrier k , $\xi_u[k]$ is the interference experienced by user u on subcarrier k and σ_n^2 is the noise power. Now, the objective function can be represented as a cost function $f(r)$ as shown in equation 21.

$$f(r) = R_{sum} = \sum_{k=1}^N \sum_{u=1}^U R_u[k] \tag{21}$$

Let $\mathbf{Z}_{u,k,t}$ represent the assignment of user u to subcarrier k during time slot t . The allocation of subcarriers and time slots is based on the available CSI for each user. Therefore, for each subcarrier k , the metric to be evaluated should be

$$\kappa_{u,k,t} = \frac{|h_u[k]^H \mathbf{W} \mathbf{F}_u[k]|^2}{\xi_u[k] + \sigma_n^2} \tag{22}$$

This metric captures the effective channel gain normalized by interference and noise. Assign time-slots and subcarriers to users with the highest effective channel gains for each subcarrier and time-slot combination. The idea is to exploit multi-user diversity by allocating resources to the users who can achieve the highest SINR in each time-slot and subcarrier. Once the time-slot and subcarrier assignment matrix \mathbf{Z} is decided, power is allocated across users and subcarriers. The water-filling

method is applied. The water-filling method is an adaptive power allocation technique that optimally distributes power across subcarriers based on channel conditions. Subcarriers with better channel gains receive more power, while those with poor channel conditions receive less, maximizing overall system capacity (Xing et al. 2020). It allocates more power to subcarriers with better channel conditions. The water-filling power allocation for user u on subcarrier k is given by

$$P_u[k] = \max \left(0, \frac{1}{\lambda} - \frac{\sigma^2}{|h_u[k]^H \mathbf{W} \mathbf{F}_u[k]|^2} \right) \tag{23}$$

where λ is a Lagrange multiplier chosen to satisfy the total power constraint for each user and $|\cdot|^H$ is the Hermitian transpose.

To avoid allocating all the best resources to just a few users, proportional fairness criterion is applied. This ensures that users with worse channel conditions still receive some

resources, maintaining a balance between maximizing throughput and ensuring fairness. The proportional fairness metric for user u on subcarrier k at time-slot t is defined as

$$\Gamma_{u,k,t} = \frac{\kappa_{u,k,t}}{R_u[k]} \tag{24}$$

Table 1: Design of Time Slot and Subcarrier Matrix

Algorithm 1: Time Slot and Subcarrier Assignment Matrix Based on Dynamic Resource Allocation

Input: $\mathbf{Z}_{u,k} = 0^{U \times K}$, ϵ , λ , $R_u = 0 \quad \forall_u \in \{1, 2, 3, \dots, U\}$

```

1  while  $R_u[n] - R_u[n-1] > \epsilon$  and  $n < N_{\max}$  do
2  for  $u \in \{1, 2, 3, \dots, U\}$ 
3  for  $k \in \{1, 2, 3, \dots, N\}$ 
4  for  $t \in \{1, 2, 3, \dots, T_C\}$ 
5   $G_{u,k} = |h_u[k]^H \mathbf{W}\mathbf{F}_u[k]|^2$  // channel gain for user  $u$  on subcarrier  $k$ 
6   $SINR_u[k] = \frac{P_u[k]G_u[k]}{\sum_{i \neq k} P_i[k]G_i[k] + \sigma^2}$ 
7   $R_u[k][t] = \log_2(1 + SINR_u[k][t])$ 
8   $(k^*, t^*) = \arg \max_{k^*, t^*} R_u[k][t]$ 
9   $\Gamma_{u,k,t} = \frac{\kappa_{u,k,t}}{R_u[k][t]}$ ;  $SINR_u[k][t] = SINR_u[k^*][t^*]$ 
10  $P_u[k][t] = \max \left( \frac{1}{\lambda} - \frac{\sigma^2}{|h_u[k]^H \mathbf{W}\mathbf{F}_u[k]|^2} \right)$ 
11  $\mathbf{Z}_{u,k,t} = \mathbf{Z}_{u,k^*,t^*}$ 
12  $R_u^n[k,t] = R_u^n[k,t] + R_u^n[k^*,t^*]$ 
13  $n \leftarrow n + 1$ 
14 end
15 end

```

It is observed in the algorithm in Table xx, that iterations proceed by updating the assignment matrix \mathbf{Z} and power allocation $P_u[k, t]$ until convergence ϵ or until the number of iterations is maximum. It is also notable that step 8 is the solution to Lagrangian function

$$L(P[k], \lambda) = \sum_{k=1}^N R_k + \lambda \left(P_{total} - \sum_{k=1}^N P[k] \right) \quad (25)$$

The objective was to maximize the sum of the achievable data rates across the subcarriers while satisfying power constraint as presented in equation 23. Therefore, taking the derivative of L with respect to $P[k]$ and set it to zero gives the optimum power allocation for each subcarrier. Equation 26 is solved numerically by bisection method.

$$\frac{\partial L}{\partial P[k]} = \frac{1}{\ln 2} \cdot \frac{1}{1 + \frac{\sigma_k^2}{P[k]|h[k]|^2}} \cdot \frac{|h[k]|^2}{\sigma_k^2} - \lambda \quad (26)$$

Hybrid Precoding Design

In Algorithm 1, the time slot and subcarrier assignment strategy has been discussed. However, the design of time slot matrix through dynamic resource allocation still requires fixing the hybrid precoder. In this part the hybrid precoding design algorithm aimed at maximizing the system's data rate is presented. Given the constraints of fixed CSI, a predetermined time-slot assignment matrix, and a fixed subcarrier power allocation, the algorithm iteratively optimizes the digital and analog precoding matrices. The goal is to ensure that the system leverages the full potential of hybrid beamforming while adapting to the underlying channel conditions. The analog precoding matrix is iteratively optimized on a manifold, where it operates in the RF domain with phase-only adjustments, while the digital precoding is updated using a

weighted minimum mean square error (MMSE) based approach. The regularization term dynamically adjusts the trade-off between maximizing the data rate and maintaining a desirable structure for the precoding matrices, ensuring stability and enhancing convergence. Convergence is achieved when the difference in the weighted sum-rate between iterations falls below a predefined threshold, indicating that the system has reached an optimal balance between performance and complexity. This refined approach allows for improved robustness in multi-carrier systems like MC-TDMA, where resource allocation and hybrid beamforming need to be tightly coordinated, particularly in the presence of channel imperfections and system constraints.

Therefore, by fixing digital precoder the problem in equation 19 can be reduced to

$$\max_{\mathbf{F}} \sum_{k=1}^N \sum_{u=1}^U R_u[k] \quad (27)$$

It is however known that for hybrid beamforming, the digital precoder design is done based on the effective channels. Hence, the effective channel matrix for all users is presented as

$$\sum_{u=1}^U \mathbf{G}_{\text{eff}}[u]^H = \mathbf{H}[u]^H \mathbf{F} \quad (28)$$

The base station usually estimates the digital precoder matrix for effective channel for minimum mean square error (MMSE) as

$$\mathbf{W}[k] = \arg \min_{\mathbf{W}} E \left[\left\| S_{RX}^k - \mathbf{W}^H h \right\|^2 \right] \quad (29)$$

The solution to the MMSE formula is given as

$$\mathbf{W}[k] = (\mathbf{H}\mathbf{H}^H + \sigma^2 \mathbf{I})\mathbf{H} \quad (30)$$

where \mathbf{I} is the identity matrix.

Now, Algorithm 2 for hybrid precoding design is presented in Table 2. The algorithm incorporates weighted regularization. Weighted regularization is used in optimization to balance performance and stability in hybrid precoding design. It introduces a penalty term that prevents

overfitting to specific channel conditions, ensuring robustness and faster convergence in practical implementations (Huang and Pan 2020). The regularization term is introduced in the objective function to smooth out the optimization landscape.

Table 2: Hybrid Precoding with Weighted Regularization Algorithm**Algorithm 2:** Hybrid Precoding with Weighted Regularization**Input:** Fixed CSI, $\mathbf{H}_u[k]$, $\mathbf{Z}_{u,k,t}$ **Initialize:** $\mathbf{F}^{(0)}$, $\mathbf{W}[k]^{(0)}$, $R_{sum}^{(0)}[k]$ convergence threshold ϵ_2 , $\beta_0 > 0$ 1 **while** $R_{sum}[n] - R_{sum}[n-1] > \epsilon_2$ and $n < N_{max}$ **do**

$$2 \quad \mathbf{F}(n) = \arg \max_{\mathbf{F}} \left[\sum_{u=1}^U \sum_{k=1}^N \log_2 \left(1 + \frac{P_u[k] |h_u[k]^H \mathbf{W}[k]^n \mathbf{F}_u[k]|^2}{\sum_{i \neq u} P_i[k] |h_i[k]^H \mathbf{W}[k]^n \mathbf{F}_i[k]|^2 + \sigma^2} \right) \right]$$

$$MMSE \mathbf{W}[k]^n = \left(\sum_{u=1}^U P_u[k] h_u[k] h_u[k]^H + \sigma^2 \mathbf{I} \right)^{-1} \cdot \sum_{u=1}^U P_u[k] h_u[k] \mathbf{F}_u[k]^n$$

3 $\beta_n = \frac{\beta_n}{1 + \Omega_n}$ where $\Omega_n > 0$ // update regularization weight4 $\mathbf{F}^{(n)} = \arg \max_{\mathbf{F}} \left[R_{sum}^n - \beta_n \|\mathbf{F}\|_{\mathbf{F}}^2 \right]$ // $\|\mathbf{F}\|^2$ is Frobenius norm of \mathbf{F} 5 $\mathbf{W}^{n+1}[k] = \arg \min_{\mathbf{W}} \left[MMSE \mathbf{W}[k]^n + \beta_n \|\mathbf{W}\|_{\mathbf{F}}^2 \right]$ 6 $R_{sum}^{n+1} = R_{sum}^{n-1} + R_{sum}^n$ 11 $n \leftarrow n + 1$ 12 **end****Experimental Results****Simulation Parameters**

In this section, the parameters for simulation analysis of the proposed joint MC-TDMA and hybrid beamforming schemes are presented. The experiments are conducted by implementing the designed algorithms to assess their effectiveness under various conditions. The proposed methods are compared with the fully digital beamformer with full channel state information and hybrid beamforming schemes presented in (Du et al. 2019) and (Shareef and Al-Kindi 2023)

The method presented in (Du et al. 2019) uses alternating optimization algorithm based on manifold optimization to maximize the performance in terms of the system spectral efficiency. In Shareef and Al-Kindi (2023) the authors used modified orthogonal matching pursuit (OMP) algorithm to design a wideband hybrid combiner based on the sparse structure of mmWave channel and OFDM. Table 3 shows the system and experimental conditions based on the 3GPP specification series TS 38.104 (Sasikumar and Jayakumari 2021) in the numerical experiments.

Table 3: Simulation and Experimental Conditions

Parameter	Value
Subcarrier spacing (Δ_f)	120 kHz
OFDM symbol duration	8.33 μ s
FFT-points N	1024
Carrier frequency	28 GHz / 60 GHz / 100 GHz
Sampling interval T_s	7.6 ns
Modulation	QPSK
CP length	72
Subcarrier mapping ($K \leq N$)	$-\frac{K}{2}, -\frac{K}{2} + 1, \dots, \frac{K}{2} - 1$
Transmission bandwidth	1 GHz 2 GHz
Users	10-100 random locations, with 16 antennas
Beamforming	64 antennas, beamwidth 10^0
Resource Allocation	Time-slot 100 μ s, water filling
Optimization Parameters	$N_{\max}=1000; \epsilon=10^{-4}$

In this work the bandwidth of transmission is assumed to be equal to the data rate. Therefore, the SINR defined in equation 18 can also be represented as

$$SINR_{dB} = 10 \log_{10} \left(\frac{E_b}{N_0} \right) \tag{31}$$

where E_b and N_0 are energy per bit and noise power spectral density. The spectral efficiency (SE) is defined in this study as the rate of data transmission per unit bandwidth. It is presented as

$$SE = \frac{1}{N} \sum_{k=1}^N \log_2(1 + SINR_k) \tag{32}$$

For simulation, 10000 random symbols are generated and the system utilizes the IDFT transform with QPSK constellations. The wideband 28 GHz channel is used divided into 1024 OFDM subchannels plus 72 cyclic prefix (CP). The right hand of equation 12 is similar to the narrowband channel model. Therefore, each user is assumed to have the same number of data streams with normal distribution. The angle of departure and complex path gains are respectively distributed as $\theta_{u,l} \sim \mathcal{U}(0, 2\pi)$ and $\alpha_{u,l} \sim \mathcal{CN}(0, 1)$.

Results and Discussion

The simulation parameters in Table 3 are used throughout the simulation experiments discussed in this section. Figure 2 depicts the

comparison of performance differences between different beamforming designs. The results of the proposed algorithms are compared to that of fully digital beamformer, the hybrid precoding for alternative optimization (HP-AO) in Du et al. (2019) and the modified orthogonal matching pursuit (OMP) in Shareef and Al-Kindi (2023). The number of BS antennas is 64, path number is fixed at 4 with eight users. The number of BS antennas, channel paths and users are represented by letters M , L and U respectively. The proposed Algorithm 1 demonstrates the best performance among all the hybrid beamforming designs. It has the smallest gap with the fully digital beamforming system of about 4dB. The HP-AO algorithm in Du et al.

(2019) outperforms the proposed when the number of channel paths is 4. However, when the number of channel paths increases to 6, Algorithm 2 performs better than HP-AO algorithm as shown in Figure 3. This verifies that the proposed algorithms are robust in

sparse channels. As the number of channel paths increases Algorithm 1 closes in to the fully digital beamforming system. This is due to the fact that the time slot and subcarrier allocation scheme optimizes the cost function with added time diversity.

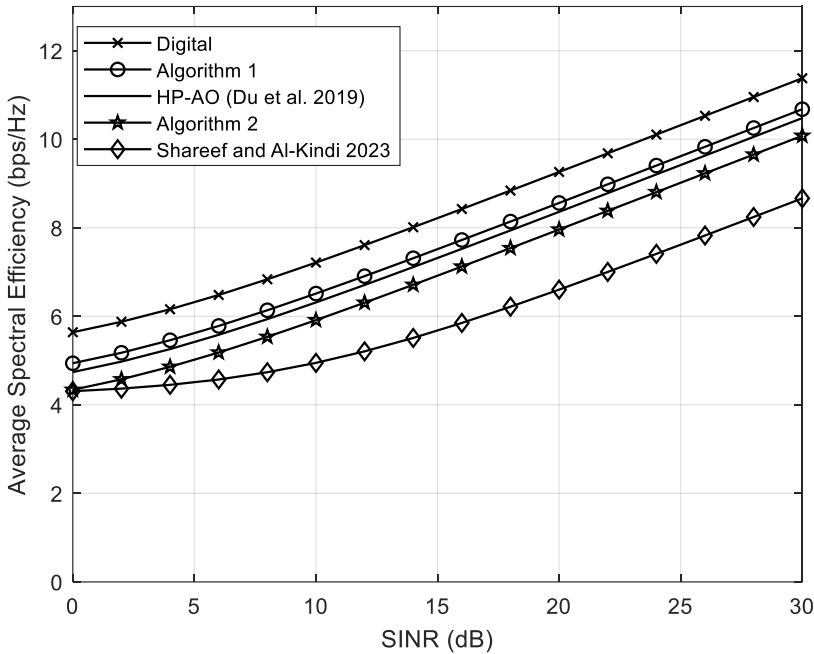


Figure 2: Spectral efficiency vs SINR with $M = 64$, $L = 4$ and $U = 8$.

Figure 4 shows the spectral efficiency performance for increased number of users. Although the performance gap between the fully digital beamforming and the HP-AO and OMP algorithms becomes larger when the number of users increases, the gap between the proposed algorithms and fully digital beamforming is still at 5dB. This demonstrates the robustness of the proposed schemes to dynamically allocate resources as the number of users grow. In Figure 5, the number of BS antennas is increased to 128 and 256 with six users. It is observed that the gap between fully digital beamforming and proposed algorithms reduces. The performance of algorithm one outperforms the existing due to the introduced time diversity. It is also observed that larger antenna array provides narrower beams, which results in higher directivity. This improves the

ability of the system to focus energy towards intended users, reducing interference and increasing the effective signal strength. Likewise, the beamforming gain is proportional to the number of antennas. As the number of antennas increases, the beamforming gain also increases, which significantly improve the system's spectral efficiency performance. This gain is observed to compensate for the for path loss in mmWave bands where high attenuation is common.

In Figure 6, it is observed that with more BS antennas, more precise beams can be directed, which reduces interference and improves signal-to-noise ratio. However, in this case the number of users is increased which necessitates the allocation of resources dynamically for optimal performance. As a

result, the spectral efficiency decreases by 2dB. But, it is observed that the amount of information transmitted per Hz improves, particularly in the case of fully digital

beamforming. In multi-user systems, more antennas allow simultaneous beamforming to multiple users (spatial multiplexing), further boosting the overall system capacity.

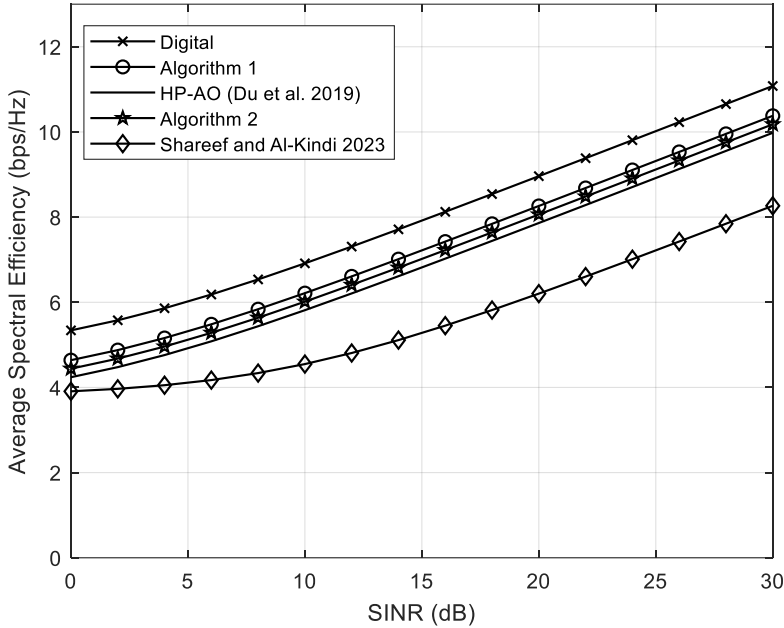


Figure 3: Spectral efficiency vs SINR with $M = 64$, $L = 6$ and $U = 8$.

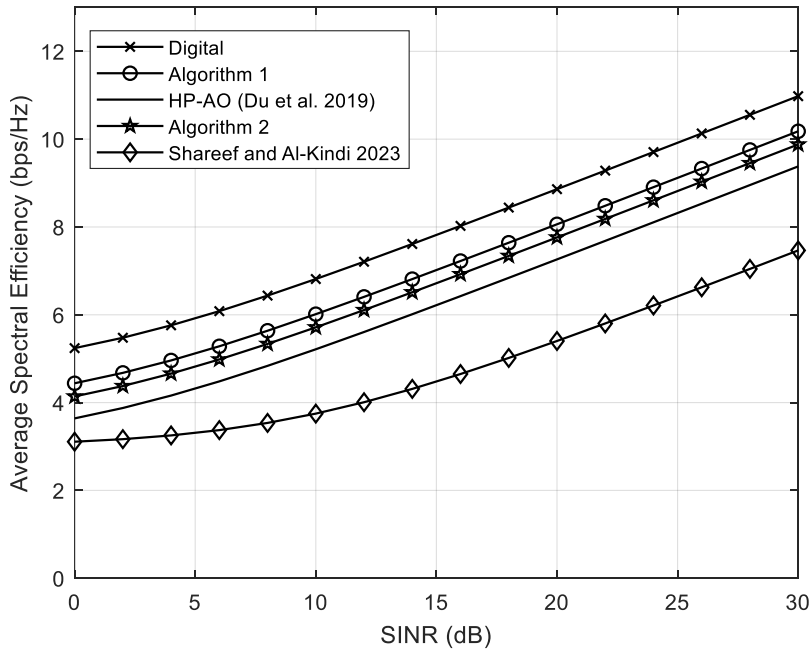


Figure 4: Spectral efficiency vs SINR with $M = 64$, $L = 4$ and $U = 16$.

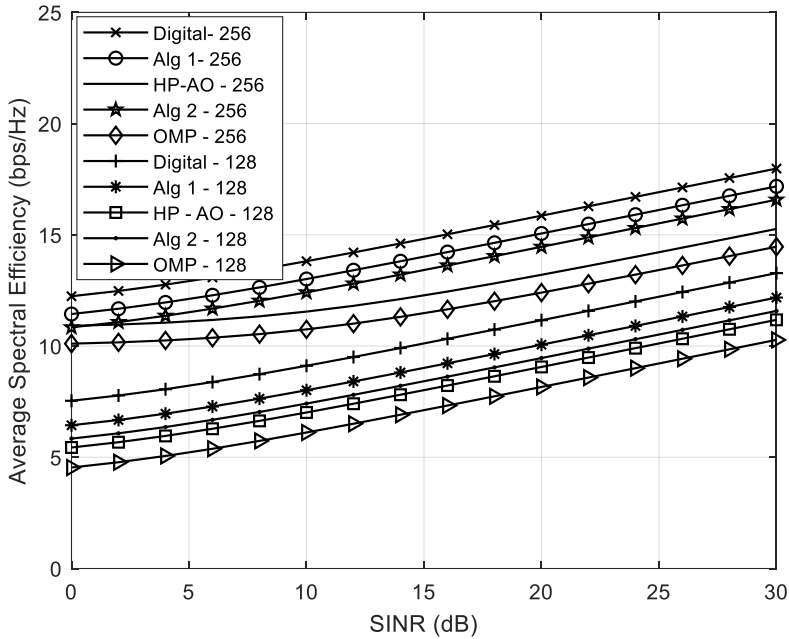


Figure 5: Spectral efficiency vs SINR with $M = 128$ and 256 , $L = 4$ and $U = 6$.

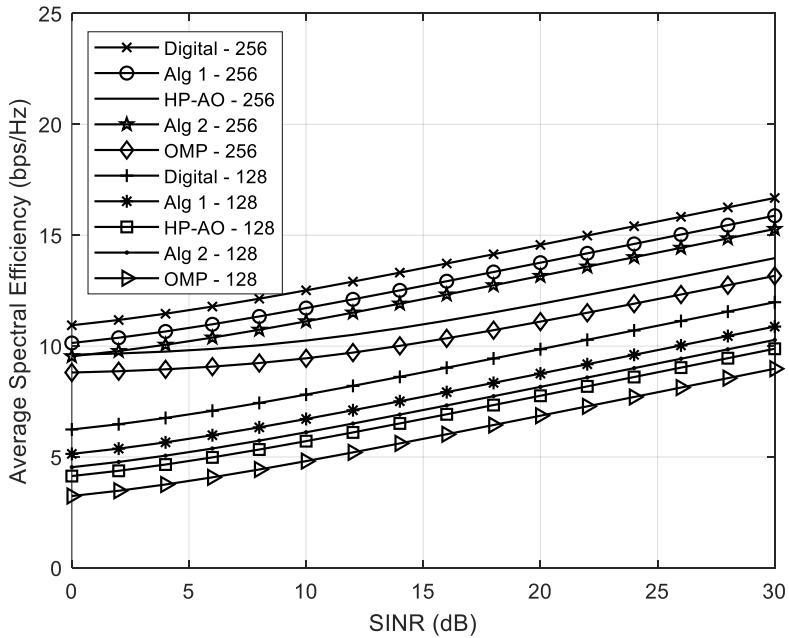


Figure 6: Spectral efficiency vs SINR with $M = 128$ and 256 , $L = 4$ and $U = 8$.

For fair comparison between proposed and existing beamforming schemes, the computational complexity is presented in Table 4. The complexity in this study is defined as of the number of multiplications, additions, matrix inversions and

computational resources needed to complete each iteration. N is the number of subcarriers, M is the number of BS antennas, N_{RF} is the number of RF chains, U is the number of users and X^{-1} represent matrix inversion.

Table 4: Complexity of Beamforming Schemes

Scheme	Complexity
Full Digital Beamforming	$O(MNUN_{RF}^U)$
Du et al., 2019	$O(NMN_{RF}^2)$
Shareef and Al-Kindi 2023	$O(MNUN_{RF}X^{-1})$
Algorithm 1	$O(MNN_{RF} + NUN_{RF})$
Algorithm 2	$O(MNUN_{RF})$

Digital beamforming system scales linearly with the number of antennas, as each antenna requires a dedicated RF chain, digital-to-analog converter (DAC), and signal processor. For large antenna arrays it results into significant increase in power consumption, processing load, and hardware costs. The computational complexity also grows due to the need for digital precoding across all antennas in real-time. The work presented in Shareef and Al-Kindi (2023) have a fair share of complexity for each iteration. This is due to the fact that the involved matrix inversion consumes computing resources extending the convergence time. The proposed schemes of Algorithm 1 and Algorithm 2 demonstrate low computation complexity compared to the existing hybrid beamforming methods. As observed in the complexity analysis in Table 4, the proposed schemes have significantly lower computational overhead compared to fully digital beamforming, making them feasible for hardware implementation in large-scale antenna systems. The iterative nature of proposed optimization algorithms ensures convergence within a reasonable number of iterations, making real-time adaptation

possible. Additionally, the proposed algorithms can be integrated with existing 5G and future 6G architectures without significant hardware modifications.

Figure 7 shows the bit error rate (BER) performance of the proposed algorithm when compared with fully digital and HP-AO beamforming system. The fully digital beamforming scheme outperformed all other beamforming schemes, indicating its superior performance due to the direct control over each antenna element, which maximizes beamforming gain and interference mitigation. The proposed Algorithm 1 followed closely, offering a balanced performance with fewer RF chains but still maintaining substantial beamforming capabilities. At a moderate SINR (e.g., 10 dB), the BER of proposed Algorithm 1 is approximately 10^{-3} , whereas the fully digital BER is around 10^{-4} , indicating a small performance gap of ~ 1 dB. At high SINR levels (20 dB+), proposed Algorithm 1 and fully digital converge, meaning the hybrid approach closely matches the performance of fully digital beamforming.

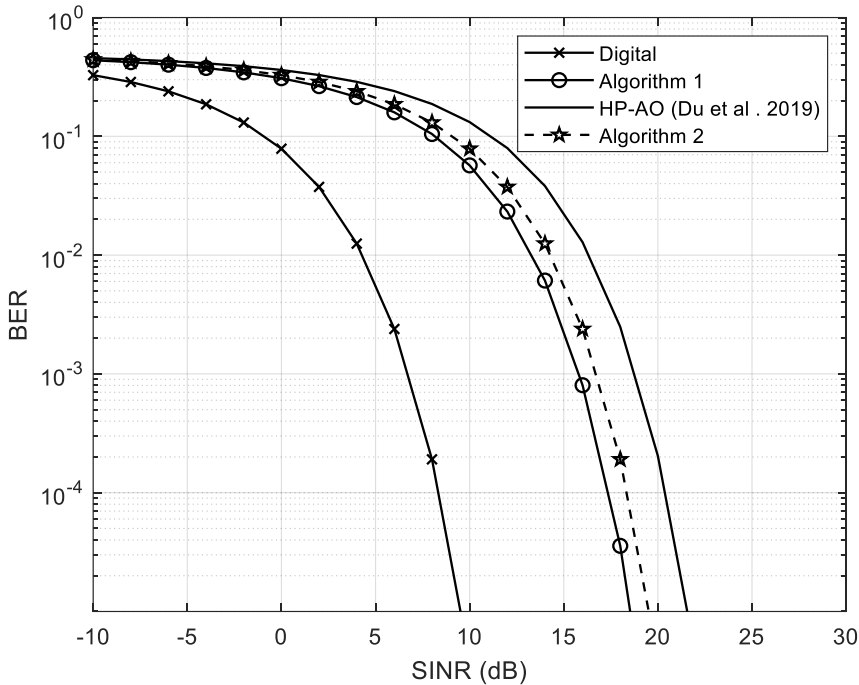


Figure 7: BER vs SINR with $M = 128$ and 256 , $L = 4$ and $U = 8$.

The proposed Algorithm 2 demonstrated moderate performance, reflecting its reduced flexibility in beamforming due to fixed time slot allocation strategy. HP-AO shows a 1-2 dB BER degradation compared to the proposed schemes, confirming its trade-off between performance and computational efficiency. The HP-AO beamforming scheme showed the least performance improvement, due to its adaptive nature that trades off efficiency for reduced complexity. These observations highlight the trade-offs between complexity and performance in beamforming architectures. Through simulation experiments done, the proposed schemes in the MC-TDMA with beamforming system, have demonstrates substantial performance improvements across various key metrics, including spectral efficiency and BER, when compared to existing techniques. The gap in spectral efficiency between the proposed hybrid schemes and the fully-digital beamforming method was minimized, particularly under realistic propagation scenarios. This highlights the effectiveness of the dynamic resource allocation and hybrid

precoding design, especially in mitigating the inherent challenges of mmWave channels, such as high path loss and interference in dense environments.

Conclusion

The problem of interest in this work was to maximize the total data rate for all users in a multi-user MC-TDMA system with hybrid beamforming, while ensuring that each user meets a minimum required signal to interference plus noise ratio (SINR). The frequency-selective nature of mmWave channels, combined with the use of time-slot and subcarrier multiplexing, posed challenges in maintaining high data rates, particularly in the presence of path loss, fading, and beam misalignment. Therefore, maximization for time slot/subcarrier allocation and hybrid precoding algorithms are presented. These schemes are based on the dynamic resource allocation. The former strives to maximize the achievable data rate by designing the time slot/subcarrier assignment matrix. The later optimizes the analog precoding matrix by updating the digital precoder using a weighted

regularization MMSE based approach. It is observed that the proposed algorithms reduce the gap to an average of 4 dB from the fully digital beamforming system when the number of BS antennas are increased from 64 to 256. The proposed algorithms have also demonstrated low complexity per iteration when compared to existing hybrid beamforming schemes. These results are integral part of modeling MC-TDMA and beamforming in the mmWave channels. By integrating MC-TDMA's flexible time-slot management with the interference mitigation and directionality of beamforming, this research addresses mmWave channels challenges, optimizing resource allocation and enhancing performance. The findings contribute to the development of efficient, next-generation networks that can handle diverse use cases, including dense urban environments and mobile user scenarios. This work offers a pathway to significantly improve the reliability and data rates of future wireless systems. While the simulations in this work are based on standardized 3GPP TS 38.104 specifications and realistic mmWave channel models, the assumptions on perfect CSI and fixed channel conditions may introduce some limitations. Future work can explore the impact of imperfect CSI and mobility on resource allocation and hybrid beamforming. Future research can also evaluate the trade-offs between performance and hardware constraints to improve deployment feasibility in large-scale 5G and 6G networks.

References

- Alkhateeb A, El Ayach O, Leus G and Heath RW 2013 Hybrid precoding for millimeter wave cellular systems with partial channel knowledge. *IEEE Inf. Theo. Appl. Workshop*. 1-5.
- Alsaedi WK, Ahmadi H, Khan Z and Grace D 2023 Spectrum Options and Allocations for 6G: A Regulatory and Standardization Review. *IEEE Open J. Commun. Soc.*. 4(1): 1787-1812.
- Bahbahani MS, Alsusa E and Hammadi A 2023 A Directional TDMA Protocol for High Throughput URLLC in mmWave Vehicular Networks. *IEEE Trans Vehicle Technol.* 72(3): 3584-3599.
- Basha AJ, Devi MR, Lokesh S, Sivaranjani P, Hussain DM and Padhy V 2023 PSO-DBNet for Peak-to-Average Power Ratio Reduction Using Deep Belief Network. *J. Com.p Syst. Sci Eng.* 45(2):1483-1493.
- Beiranvand J, Nguyen MD, Meghdadi V, Menudier C and Cancès JP 2023 Hybrid Beamforming with Fixed Phase Shifters in OFDM-Based Multiuser MISO Systems. *IEEE Glob Commun. Conf.* 5841-5846.
- Busari SA, Huq KMS, Mumtaz S, Dai L and Rodriguez J 2018 Millimeter-Wave Massive MIMO Communication for Future Wireless Systems: A Survey. *IEEE Comm Surveys Tutorials*. 20(2): 836-869.
- Chen L, Nooshabadi S, Khoeiini F, Khalifa Z, Hadidian B, and Afshari E 2021 An ultra-fast frequency shift mechanism for high data-rate sub-THz wireless communications in CMOS. *Appl. Phys. Lett.* 118(24): 242103.
- Chen W, Lin X, Lee J, Toskala A, Sun S, Chiasserini CF and Liu L 2023 5G-Advanced Toward 6G: Past, Present, and Future. *IEEE J. Select. Areas Commun.* 41(6): 1592-1619.
- Chen Wenrong, Li L, Chen Z, Quek T and Li S 2022 Enhancing THz/mmWave Network Beam Alignment With Integrated Sensing and Communication. *IEEE Commun. Lett.* 26(7). 1698-1702.
- Du J, Xu W, Zhao C and Vandendorpe L 2019 Weighted Spectral Efficiency Optimization for Hybrid Beamforming in Multiuser Massive MIMO-OFDM Systems. *IEEE Trans Vehicle Technol.* 68(10). 9698-9712.
- Eisenbeis J, Kern N, Tingulstad M, Giroto De Oliveira L and Zwick T 2021 Sparse Array Channel Estimation for Subarray-Based Hybrid Beamforming Systems. *IEEE Wireless Commun. Lett.* 10(2). 231-235.
- Farhang-Boroujeny B 2011 OFDM versus filter bank multicarrier. *IEEE Sign. Proc. Magazine*. 28(3). 92-112.
- Getahun H and Rajkumar S 2023 Performance analysis of mmWave radio propagations in an indoor environment for 5G networks. *Eng. Res. Express*. 5(2). 1-25.
- Golos E, Daraseliya A, Sopin E, Begishev V and Gaidamaka Y 2023 Optimizing Service

- Areas in 6G mmWave/THz Systems with Dual Blockage and Micromobility. *Mathematics*. 11(4). 1-13.
- Hamid S, Chopra SR, Gupta A, Tanwar S, Florea BC, Taralunga DD, Alfarraj O and Shehata AM 2023 Hybrid Beamforming in Massive MIMO for Next-Generation Communication Technology. *Sensors*. 23(16). 7294.
- Huang Y, Hu S and Wu G 2023 A TDMA approach for OFDM-based multiuser RadCom systems. *China Commun*. 20(5). 93-103.
- Huang Z and Pan A 2020 Non-local weighted regularization for optical flow estimation. *Optik*. 208(4). 164069.
- Ji H, Park S, Yeo J, Kim Y, Lee J and Shim B 2018 Ultra-Reliable and Low-Latency Communications in 5G Downlink: Physical Layer Aspects. *IEEE Wireless Commun*. 25(3). 124-130.
- Khaled I, Falou A El, Langlais C, Jezequel M and Elhassan B 2023 Angle-Domain Hybrid Beamforming-Based mmWave Massive MIMO-NOMA Systems. *IEEE Open J. Commun. Soc*. 4(1). 684-699.
- Khudhair SA and Singh MJ 2021 Performance evaluation of the use of filter bank multi-carrier waveform in different Mmwave frequency bands. *J. of Comms*. 16(1). 36-41.
- Kutty S and Sen D 2016 Beamforming for Millimeter Wave Communications: An Inclusive Survey. *IEEE Comms. Surveys Tutorials*. 18(2). 949-973.
- Li J, Niu Y, Wu H, Ai B, Chen S, Feng Z, Zhong Z and Wang N 2022 Mobility Support for Millimeter Wave Communications: Opportunities and Challenges. *IEEE Commun. Surveys Tutorials*. 24(3). 1816-1842.
- Mezzavilla M, Zhang M, Polese M, Ford R, Dutta S, Rangan S and Zorzi M 2018 End-to-end simulation of 5G mmWave networks. *IEEE Commun. Surveys Tutor*. 20(3). 2237-2263.
- Moltchanov D, Sopin E, Begishev V, Samuylov A, Koucheryavy Y and Samouylov K 2022 A Tutorial on Mathematical Modeling of 5G/6G Millimeter Wave and Terahertz Cellular Systems. *IEEE Commun. Surveys Tutorials*. 24(2). 1072-1116.
- Naik MN and Virani HG 2022 A compact four port MIMO antenna for millimeterwave applications. *Bull. Electr. Eng. Informatics*. 11(2). 878-885.
- Raheja DK, Kanaujia BK and Kumar S 2019 Compact four-port MIMO antenna on slotted-edge substrate with dual-band rejection characteristics. *Int. J. RF Microwave Comput Aided Eng*. 29(7). 1-15.
- Rajashekar R, Xu C, Ishikawa N, Yang LL and Hanzo L 2019 Multicarrier division duplex aided millimeter wave communications. *IEEE Access*. 7(1). 100719-100732.
- Rappaport TS, MacCartney GR, Samimi MK and Sun S 2015 Wideband millimeter-wave propagation measurements and channel models for future wireless communication system design. *IEEE Trans. Commun*. 63(9). 3029-3056.
- Sasikumar S and Jayakumari J 2021 Genetic algorithm-based joint Spectral-Energy efficiency optimisation for 5G heterogeneous network. *Int. J. Electronics*. 108(6). 887-907.
- Shareef FF and Al-Kindi MJ 2023 OFDM-based Wideband Hybrid Beamformer for mmWave Massive MIMO Multiuser 5G Systems. *Bull. Electric. Eng. Inf*. 12(3). 1486-1494.
- Sohrabi F and Yu W 2017 Hybrid Analog and Digital Beamforming for mmWave OFDM Large-Scale Antenna Arrays. *IEEE J. Select. Areas Commun*. 35(7). 1432-1443.
- Song X, Kuhne T and Caire G 2020 Fully-partially-connected hybrid beamforming architectures for mmWave MU-MIMO. *IEEE Trans. Wireless Commun*. 19(3). 1754-1769.
- Soumya A, Krishna Mohan C and Cenkeramaddi LR 2023 Recent Advances in mmWave-Radar-Based Sensing, Its Applications, and Machine Learning Techniques: A Review. *Sensors*. 23(21). 8901.
- Teng Y, Jia L, Liu A, and Lau VKN 2021 A Hybrid Pilot Beamforming and Channel Tracking Scheme for Massive MIMO Systems. *IEEE Trans. Wireless Commun*. 20(9). 6078-6092.
- Ullah MS, Sarker SC, Ashraf Z Bin and Uddin

- MF 2022 Spectral Efficiency of Multiuser Massive MIMO-OFDM THz Wireless Systems with Hybrid Beamforming under Inter-carrier Interference. *Int. Conf. Electr. Comput. Eng.* 228-231.
- Verma S and Mishra S 2022 Miniature Diamond-Shaped Millimeterwave Antenna Array for 5G Applications. *Asian Conf. Innovat. Technol.* 1-5.
- Wang YY, Chen BR and Hsu CH 2023 Efficient Maximum Likelihood Algorithm for Estimating Carrier Frequency Offset of Generalized Frequency Division Multiplexing Systems. *Mathematics.* 11(15). 3426.
- Xing C, Jing Y, Wang S, Ma S and Poor HV 2020 New viewpoint and algorithms for water-filling solutions in wireless communications. *IEEE Trans. Signal Process.* 68(1). 1618-1634.
- Xue Q, Ji C, Ma S, Guo J, Xu Y, Chen Q and Zhang W 2024 A Survey of Beam Management for mmWave and THz Communications Towards 6G. *IEEE Comms. Surveys Tutor.* 26(3). 1520-1559.
- Yong WY, Vosoogh A, Bagheri A, Van De Ven C, Hadaddi A and Glazunov AA 2023 An Overview of Recent Development of the Gap-Waveguide Technology for mmWave and Sub-THz Applications. *IEEE Access.* 11(1). 69378-69400.
- Yuan M, Wang H, Yin H and He D 2023 Alternating Optimization Based Hybrid Transceiver Designs for Wideband Millimeter-Wave Massive Multiuser MIMO-OFDM Systems. *IEEE Trans. Wireless Commun.* 22(12). 9201-9217.
- Yusof A, Idris A and Abdullah E 2023 Paper reduction in cp-ofdm (5g) using hybrid technique. *Acta Polytechnica.* 63(5). 364-370.
- Zhang T and Zhu Q 2020 EVC-TDMA: An enhanced TDMA based cooperative MAC protocol for vehicular networks. *J. Commun. Networks.* 22(4). 316-325.